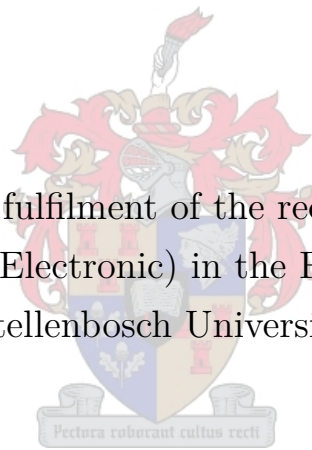# Data-Driven System Identification etc

Luke Skywalker

99652154

Thesis presented in partial fulfilment of the requirements for the degree of Master of Engineering (Electronic) in the Faculty of Engineering at Stellenbosch University.

Supervisor: Dr O. W. Kenobi

Department of Electrical and Electronic Engineering

October 2099

Acknowledgements

I would like to thank my dog, Muffin. I also would like to thank the inventor of the incubator; without him/her, I would not be here. Finally, I would like to thank Dr Herman Kamper for this amazing report template.

Plagiaatverklaring / *Plagiarism Declaration*

1. Plagiaat is die oorneem en gebruik van die idees, materiaal en ander intellektuele eiendom van ander persone asof dit jou eie werk is.

   Plagiarism is the use of ideas, material and other intellectual property of another's work and to present is as my own.

2. Ek erken dat die pleeg van plagiaat 'n strafbare oortreding is aangesien dit 'n vorm van diefstal is.

   I agree that plagiarism is a punishable offence because it constitutes theft.

3. Ek verstaan ook dat direkte vertalings plagiaat is.

   I also understand that direct translations are plagiarism.

4. Dienooreenkomstig is alle aanhalings en bydraes vanuit enige bron (ingesluit die internet) volledig verwys (erken). Ek erken dat die woordelikse aanhaal van teks sonder aanhalingstekens (selfs al word die bron volledig erken) plagiaat is.

   Accordingly all quotations and contributions from any source whatsoever (including the internet) have been cited fully. I understand that the reproduction of text without quotation marks (even when the source is cited) is plagiarism

5. Ek verklaar dat die werk in hierdie skryfstuk vervat, behalwe waar anders aangedui, my eie oorspronklike werk is en dat ek dit nie vantevore in die geheel of gedeeltelik ingehandig het vir bepunting in hierdie module/werkstuk of 'n ander module/werkstuk nie.

   I declare that the work contained in this assignment, except where otherwise stated, is my original work and that I have not previously (in its entirety or in part) submitted it for grading in this module/assignment or another module/assignment.

Studentenommer / *Student number*	Handtekening / *Signature*
Voorletters en van / *Initials and surname*	Datum / *Date*

Abstract

English

The English abstract.

Afrikaans

Die Afrikaanse uittreksel.

Contents

List of Figures

List of Tables

Nomenclature

Variables and functions

$p(x)$	Probability density function with respect to variable x.
$P(A)$	Probability of event A occurring.
ε	The Bayes error.
ε_u	The Bhattacharyya bound.
B	The Bhattacharyya distance.
s	An HMM state. A subscript is used to refer to a particular state, e.g. s_i refers to the ith state of an HMM.
$\mathbf{S}$	A set of HMM states.
$\mathbf{F}$	A set of frames.
$\mathbf{o}_f$	Observation (feature) vector associated with frame f.
$\gamma_s(\mathbf{o}_f)$	A posteriori probability of the observation vector $\mathbf{o}_f$ being generated by HMM state s.
μ	Statistical mean vector.
Σ	Statistical covariance matrix.
$L(\mathbf{S})$	Log likelihood of the set of HMM states $\mathbf{S}$ generating the training set observation vectors assigned to the states in that set.
$\mathcal{N}(\mathbf{x}|\mu, \Sigma)$	Multivariate Gaussian PDF with mean μ and covariance matrix Σ.
a_{ij}	The probability of a transition from HMM state s_i to state s_j.
N	Total number of frames or number of tokens, depending on the context.
D	Number of deletion errors.
I	Number of insertion errors.
S	Number of substitution errors.

Acronyms and abbreviations

AE	Afrikaans English
AID	accent identification
ASR	automatic speech recognition
AST	African Speech Technology
CE	Cape Flats English
DCD	dialect-context-dependent
DNN	deep neural network
G2P	grapheme-to-phoneme
GMM	Gaussian mixture model
HMM	hidden Markov model
HTK	Hidden Markov Model Toolkit
IE	Indian South African English
IPA	International Phonetic Alphabet
LM	language model
LMS	language model scaling factor
MFCC	Mel-frequency cepstral coefficient
MLLR	maximum likelihood linear regression
OOV	out-of-vocabulary
PD	pronunciation dictionary
PDF	probability density function
SAE	South African English
SAMPA	Speech Assessment Methods Phonetic Alphabet

Chapter 1

Introduction

The last few years have seen great advances in speech recognition. Much of this progress is due to the resurgence of neural networks; most speech systems now rely on deep neural networks (DNNs) with millions of parameters [**?**, **?**]. However, as the complexity of these models has grown, so has their reliance on labelled training data. Currently, system development requires large corpora of transcribed speech audio data, texts for language modelling, and pronunciation dictionaries. Despite speech applications becoming available in more languages, it is hard to imagine that resource collection at the required scale would be possible for all 7000 languages spoken in the world today.

I really like apples.

1.1. Section heading

Chapter 2

Modelling

This chapter discusses the mathematical modelling of a quadrotor with a suspended payload which is based on a practical quadrotor UAV named Honeybee. The model is first derived as a 2D model. The system identification and control system techniques in later chapters will then be explained based on the 2D model to avoid unnecessary complexity. Finally, it will be described how this model and the techniques in later chapters are extended to the 3D case. This 3D mathematical model will be used in a nonlinear simulation of a quadrotor and suspended payload.

2.1. Coordinate frames

2.2. States

2.3. Forces and moments

2.4. Lagrangian mechanics

2.5. Linearised model

2.6. Discretised model

2.7. Model verification

2.8. Dynamic payloads

Chapter 3

System identification

System identification is the process of creating mathematical models of a dynamical system by using input and output measurements of that system. Two major approaches are used to represent the dynamics of such a system:

1. A priori mathematical modelling with parameter estimation

2. Data-driven system identification

Models determined from a priori modelling and parameter estimation are referred to as white-box models. In contrast, data-driven system identification methods result in black-box models. This chapter discusses these system identification approaches and describes the differences between them. For each approach, different estimation techniques are explained and applied to the quadrotor and payload system. The results of these techniques are then compared to each other.

3.1. White-box and black-box techniques

3.1.1. White-box techniques

The underlying physics of a white-box model is understood by the user because they are determined from first principles. This is done by modelling physical processes with techniques like Lagrangian mechanics or Newton equations. With system identification techniques that use these models, the mathematical relations between system parameters are predefined in the modelling phase. The system identification process is therefore reduced to parameter estimation to determine values for parameters used in die model.

This approach is used by [?] and [?] for swing damping control of a quadrotor with an unknown suspended payload. The system was modelled as two rigid bodies connected by a link and the following assumptions were made regarding the suspended payload:

- The payload is a point mass.

- The link is massless.

- The link is rigid.

- The link is attached to the CoM of the quadrotor.

The only unknown parameters in the quadrotor and payload model is the payload mass and link length. These parameters are first estimated and then inserted into the predefined, linearised model. This model is used by a LQR controller to damp swing angles while also controlling the vehicle.

The approach works well for systems with predictable dynamics, but it is not very adaptable. The payload considered by [**?**] and [**?**] is limited to a small rigid mass suspended from the quadrotor by a non-stretching cable. In this use case it was shown that a LQR controller successfully controls a quadrotor while minimising payload swing angles. However, if a payload or cable is used that violates one of the modelling assumptions, the predefined model no longer accurately represent the system. Since the controller is dependent on this model, the mismatch between the model and actual dynamics may result in undesirable controller behaviour.

3.1.2. Black-box techniques

Data-driven system identification methods produce black-box models. In contrast to white-box models, black-box models do not require predefined mathematical relations between system parameters. No prior knowledge of the physics of the system are considered and no modelling assumptions are made. Black-box techniques determine the mathematical relationship between inputs and outputs of a system using information from measurement data only.

Black-box models can be categorised as either non-linear or linear models. Non-linear models are often more accurate than linear models because complex, real-world dynamics are better approximated by non-linear systems. The dynamics of a quadrotor and suspended payload are also non-linear. Examples of black box models with quadrotors and payloads in literature ???

However, non-linear models are inherently more complex than linear models. Controllers that use non-linear models are usually more computationally complex than those with linear models. Control archetictures for quadrotors used in practical applications are mostly implemented on onboard hardware. Therefore there is value in low-complexity, linear models since these may be simple enough to execute on low cost hardware. trade-off between accuracy and complexity. Non-linear models may require control implementations that are too computationally expensive and may not be practically realisable on the available hardware on a quadrotor.

DMDc and HAVOK are the two data-driven system identification methods investigated in this paper. These are linear regression techniques that produce a linear model to approximate non-linear dynamics. Non-linear data-driven techniques like Neural Networks and SINDy [**?**] may produce models that are more accurate than linear techniques, but at the cost of greater computational complexity. Name more techniques DMDc and HAVOK are less computationally complex and their models are suitable for linear MPC, which is significantly faster than non-linear MPC. This is desirable for the quadrotor use case, where onboard computational power is limited.

These techniques and their implementation are explained in the sections below. Each technique is considered for use in a velocity controller in the North direction

Considered controller The model identified by DMDc will be used to design a longitudinal velocity controller. As shown in **??**, the plant considered for system identification includes the dynamics of the inner loop, attitude controllers. The swing damping controllers which will utilise the identified model act only in the translational velocity loop. Because of the large time-scale separation between the inner and outer loop controllers, the attitude states have a negilable effect on the plant dynamics seen by the velocity controller. As discussed in Section **??**, the payload minimally effects the quadrotor attitude because it is attached near the CoM of the vehicle. Therefore the attitude states are excluded from the system identification model.

3.2. Plant considered for system identification

Derived model Figure **??** shows the plant considered for system identification. In Chapter **??** the differential equations that describe the motion of this system are derived with Lagrangian mechanics. From these equations it is clear that the considered plant is defined by the state vector,

$$\boldsymbol{x} = \begin{bmatrix} V_N & \dot{\theta} \end{bmatrix}^T, \tag{3.1}$$

and the input vector,

$$\boldsymbol{u} = \begin{bmatrix} A_{N,sp} \end{bmatrix}, \tag{3.2}$$

3.3. Parameter estimation

3.3.1. Predetermined linear model

The motivation for paramater estimation is to determine unknown parameter values required by the predetermined model. This model was derived a prioiri in Section **??**.
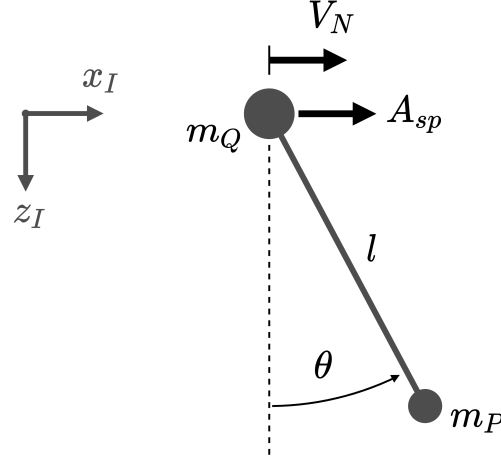
Figure 3.1: Floating pendulum model considered for system identification for a North velocity controller

3.3.2. Payload mass estimation

RLS

3.3.3. Cable length estimation

The cable length is estimated from the measurement of natural frequency of the swinging payload. As described by [**?**], the natural frequency is given by:

$$\omega_n = \sqrt{\frac{g}{l} \cdot \frac{m_q + m_p}{m_q}} \tag{3.3}$$

The natural frequency is measured by performing a FFT on the payload swing angle response after a position step by the quadrotor. The dominant frequency identified by the FFT during free swing is the natural frequency of the payload.

?? shows the payload swing angle after the system is stimulated by a position step setpoint. As shown in **??** the first few seconds of the step response are not used in the FFT. This is to minimise the effect of the quadrotor controllers on the swing angle frequency by excluding the transient response in the FFT.

?? shows the resulting amplitude spectrum of the payload swing angle response. The dominant frequency is clearly identified as ??. Since m_q and g is known, and m_p and ω_n has been estimated, l can now be determined from **??**. In this case the estimated length is ??, compared to the actual length of ??.

Frequency resolution ?? error for different lengths??

3.4. Dynamic Mode Decomposition with control

Intro DMD is a linear regression technique that can be used to approximate a non-linear dynamical system [**?**]. It uses temporal measurements of system outputs to reconstruct system dynamics without prior modelling assumptions. DMDc is an adaptation of DMD that also accounts for control inputs [**?**]. This section provides an overview of the specific implementation of DMDc used in this paper. Note that this implementation is a slight adaptation of DMDc, and includes time-delay-embedding of multiple observables. [**?**] and [**?**] use time-delay-embedding in their DMD adaptions in similar ways.

State space model DMD produces a linear, discrete state-space model of the system dynamics. Discrete measurements, $\boldsymbol{x}_k$, of the continuous time observable, $\boldsymbol{x}(t)$, are used, where $\boldsymbol{x}_k = \boldsymbol{x}(kT_s)$, and T_s is the sampling time of the model. Delay-coordinates (i.e. $\boldsymbol{x}_{k-1}, \boldsymbol{x}_{k-2}$, etc.) are also included in the state-space model to account for input delay and state delay in the system. Input delay refers to the time delay involved with transporting a control signal to a system, whereas state delay refers to time-separated interactions between system variables [**?**]. Hence, we define an state delay vector as:

$$\boldsymbol{d}_k = \begin{bmatrix} \boldsymbol{x}_{k-1} & \boldsymbol{x}_{k-2} & \cdots & \boldsymbol{x}_{k-q} \end{bmatrix}^T, \tag{3.4}$$

$\boldsymbol{d}_k \in \mathbb{R}^{(n_x)(q)}$ and where q is the number of delay-coordinates used in the model.

The discrete state-space model is therefore defined as:

$$\boldsymbol{x}_{k+1} = \boldsymbol{A}\boldsymbol{x}_k + \boldsymbol{A}_d\boldsymbol{d}_k + \boldsymbol{B}\boldsymbol{u}_k, \tag{3.5}$$

$\boldsymbol{A} \in \mathbb{R}^{n_x \times n_x}$ is the system matrix, $\boldsymbol{A}_1 \in \mathbb{R}^{(q \cdot n_x) \times (q \cdot n_x)}$ is the state delay system matrix and $\boldsymbol{B} \in \mathbb{R}^{n_x \times n_u}$ is the input matrix.

Training data The training data consists of full-state measurements, $\boldsymbol{x}_k$, and corresponding inputs, $\boldsymbol{u}_k$, taken at regular intervals of $\Delta t = T_s$, during a simulated flight with Cascaded PID control. In a practical flight, these time-series measurements need to be saved in memory because it is usd as a single batch by DMD. Note that DMD can be applied in a recursive manner as described in [**?**], However this implementation is not considered because memory size will not be a limitation since a companion computer will be used.

Data matrices The training data is collected into the following matrices:

$$
\begin{aligned}
\boldsymbol{X}' &= \begin{bmatrix} \boldsymbol{x}_{q+2} & \boldsymbol{x}_{q+3} & \boldsymbol{x}_{q+4} & \cdots & \boldsymbol{x}_{w+q+1} \end{bmatrix}, \\
\boldsymbol{X} &= \begin{bmatrix} \boldsymbol{x}_{q+1} & \boldsymbol{x}_{q+2} & \boldsymbol{x}_{q+3} & \cdots & \boldsymbol{x}_{w+q} \end{bmatrix}, \\
\boldsymbol{X}_d &= \begin{bmatrix} \boldsymbol{x}_q & \boldsymbol{x}_{q+1} & \boldsymbol{x}_{q+2} & \cdots & \boldsymbol{x}_{w+q-1} \\ \vdots & \vdots & \vdots & \ddots & \vdots \\ \boldsymbol{x}_2 & \boldsymbol{x}_3 & \boldsymbol{x}_4 & \cdots & \boldsymbol{x}_{w+1} \\ \boldsymbol{x}_1 & \boldsymbol{x}_2 & \boldsymbol{x}_3 & \cdots & \boldsymbol{x}_w \end{bmatrix}, \\
\boldsymbol{\Upsilon} &= \begin{bmatrix} \boldsymbol{u}_q & \boldsymbol{u}_{q+1} & \boldsymbol{u}_{q+2} & \cdots & \boldsymbol{u}_{w+q-1} \end{bmatrix},
\end{aligned}
\tag{3.6}
$$

where w is the number of columns in the matrices, $\boldsymbol{X}'$ is the matrix $\boldsymbol{X}$ shifted forward by one time-step, $\boldsymbol{X}_d$ is the matrix with delay states, and $\boldsymbol{\Upsilon}$ is the matrix of inputs. Equation (**??**) can be combined with the matrices in Equation (**??**) to produce:

$$
\boldsymbol{X}' = \boldsymbol{A}\boldsymbol{X} + \boldsymbol{A}_d\boldsymbol{X}_d + \boldsymbol{B}\boldsymbol{\Upsilon}.
\tag{3.7}
$$

Note that the primary objective of DMDc is to determine the best fit model matrices, $\boldsymbol{A}$, $\boldsymbol{A}_d$ and $\boldsymbol{B}$, given the data in $\boldsymbol{X}'$, $\boldsymbol{X}$, $\boldsymbol{X}_d$, and $\boldsymbol{\Upsilon}$ [**?**]. In order to group the unknowns into a single matrix, (**??**) is manipulated into the form,

$$
\boldsymbol{X}' = \begin{bmatrix} \boldsymbol{A} & \boldsymbol{A}_d & \boldsymbol{B} \end{bmatrix} \begin{bmatrix} \boldsymbol{X} \\ \boldsymbol{X}_d \\ \boldsymbol{\Upsilon} \end{bmatrix} = \boldsymbol{G}\boldsymbol{\Omega},
\tag{3.8}
$$

where $\boldsymbol{\Omega}$ contains the state and control data, and $\boldsymbol{G}$ represents the system and input matrices.

SVD A SVD is performed on $\boldsymbol{\Omega}$ resulting in: $\boldsymbol{\Omega} = \boldsymbol{U}\boldsymbol{\Sigma}\boldsymbol{V}^T$. Often, only the first p columns of $\boldsymbol{U}$ and $\boldsymbol{V}$ are required for a good approximation of the dynamics [**?**]. In many cases, the truncated form results in better models than the exact form when noisy measurements are used. This is because the effect of measurement noise is mostly captured by the truncated columns of $\boldsymbol{U}$ and $\boldsymbol{V}$. By truncating these columns, the influence of noise in the regression problem is reduced. explain this better hence the SVD is used in the truncated form:

$$
\boldsymbol{\Omega} \approx \tilde{\boldsymbol{U}}\tilde{\boldsymbol{\Sigma}}\tilde{\boldsymbol{V}}^T,
\tag{3.9}
$$

where ˜ represents rank-p truncation. maybe insert colour pictures showing matrices

By combining (**??**) with the over-constrained equality in (**??**), the least-squared solution, $\boldsymbol{G}$, can be found with:

$$\boldsymbol{G} \approx \boldsymbol{X}'\tilde{\boldsymbol{V}}\tilde{\boldsymbol{\Sigma}}^{-1}\tilde{\boldsymbol{U}}. \tag{3.10}$$

By reversing **??**, $\boldsymbol{G}$ can now be separated into: $\boldsymbol{G} = \begin{bmatrix} \boldsymbol{A} & \boldsymbol{A}_d & \boldsymbol{B} \end{bmatrix}$. according to the required dimensions of each matrix. Thereby, the state-space model approximated by DMDc is complete.

3.5. Hankel Alternative View Of Koopman

q = number of delays, from here up

HAVOK is a data-driven, regression technique that provides a connection between DMD and Koopman operator theory [**?**, **?**]. We have adapted the standard HAVOK algorithm slightly to account for the effect of control and to extract a discrete, linear model that approximates the behaviour of a controlled dynamical system. In this section, a brief overview is provided for this implementation and expansion of HAVOK.

The extracted discrete state-space model is defined as:

$$\boldsymbol{a}_{k+1} = \tilde{\boldsymbol{A}}\boldsymbol{a}_k + \tilde{\boldsymbol{B}}\boldsymbol{u}_k, \tag{3.11}$$

where $\boldsymbol{a}_k$ is the state vector previously defined in Section **??**, $\tilde{\boldsymbol{A}} \in \mathbb{R}^{(q \cdot n_x) \times (q \cdot n_x)}$ is the system matrix, and $\tilde{\boldsymbol{B}} \in \mathbb{R}^{(q \cdot n_x) \times n_u}$ is the input matrix. Here, ˜ is used to differentiate these matrices from $\boldsymbol{A}$ and $\boldsymbol{B}$ used in DMDc.

The original HAVOK algorithm, developed by [**?**], constructs a Hankel matrix from output variables only. In order to incorporate the effect of control, an extended Hankel matrix, $\boldsymbol{\Pi}$, is created by appending a matrix of inputs to a Hankel matrix of measurements:

$$\boldsymbol{\Pi} = \begin{bmatrix} \boldsymbol{a}_q & \boldsymbol{a}_{q+1} & \boldsymbol{a}_{q+2} & \cdots & \boldsymbol{a}_{w+q-1} \\ \boldsymbol{u}_q & \boldsymbol{u}_{q+1} & \boldsymbol{u}_{q+2} & \cdots & \boldsymbol{u}_{w+q-1} \end{bmatrix}, \tag{3.12}$$

where w is the number of columns in $\boldsymbol{\Pi}$. A truncated SVD of this Hankel matrix results in following approximation:

$$\boldsymbol{\Pi} \approx \tilde{\boldsymbol{U}}\tilde{\boldsymbol{\Sigma}}\tilde{\boldsymbol{V}}^T, \tag{3.13}$$

where ˜ represents rank-p truncation. It is important to note that the model extracted by HAVOK depends on the choice of hyperparameters, p and q. The number of samples in the training data, $N_{train} = w + q - 1$, also influences the accuracy of the model.

The columns of $\tilde{V}$ are the most significant principal components of the system dynamics [**?**]. This matrix, $\tilde{V}$, can be considered to contain a time-series of the pseudo-state, v, such that $\tilde{V}^T = \begin{bmatrix} v_q & v_{q+1} & \cdots & v_w \end{bmatrix}$, characterises the evolution of the actual dynamics in an eigen-time-delay coordinate system [**?**]. Consider the following discrete, state-space formulation:

$$v_{k+1} = \Lambda v_k. \tag{3.14}$$

Recall that DMDc finds a best fit linear operator that directly maps a_k to a_{k+1}. Similarly, HAVOK determines the best fit linear operator Λ that maps the pseudo-state v_k to v_{k+1}. So, in order to setup an over-determined equality for (**??**), $\tilde{V}^T$ is divided into two matrices:

$$
\begin{aligned}
V_1 &= \begin{bmatrix} v_q & v_{q+1} & ... & v_{w-1} \end{bmatrix}, \\
V_2 &= \begin{bmatrix} v_{q+1} & v_{q+2} & ... & v_w \end{bmatrix},
\end{aligned} \tag{3.15}
$$

where V_2 is V_1 advanced a single step forward in time. The matrices from Equation (**??**) are now combined with Equation (**??**) and the best fit Λ is determined with the Moore-Penrose pseudoinverse:

$$V_2 = \Lambda V_1 \qquad \Rightarrow \qquad \Lambda \approx V_1 V_1^\dagger \tag{3.16}$$

It can be shown from Equation (**??**) that Equation (**??**) is transformed from the eigen-time-delay coordinate system to the original coordinate system as the following:

$$\begin{bmatrix} a_{k+1} \\ u_{k+1} \end{bmatrix} = (\tilde{U}\tilde{\Sigma})\Lambda(\tilde{U}\tilde{\Sigma})^\dagger \begin{bmatrix} a_k \\ u_k \end{bmatrix}. \tag{3.17}$$

This form is used to extract $\tilde{A}$ and $\tilde{B}$ from the matrix, $(\tilde{U}\tilde{\Sigma})\Lambda(\tilde{U}\tilde{\Sigma})^\dagger$, in the following way:

$$\begin{bmatrix} a_{k+1} \\ u_{k+1} \end{bmatrix} = \begin{bmatrix} \tilde{A} & \tilde{B} \\ \textit{(discarded)} \end{bmatrix} \begin{bmatrix} a_k \\ u_k \end{bmatrix}. \tag{3.18}$$

Note that the matrix entries in (**??**) that map u_k to u_{k+1} are meaningless for our purposes and are discarded. Similarly to DMDc, some matrix entries in $\tilde{A}$ and $\tilde{B}$ are known a priori due to the relative positions of delay coordinates. These are forced to 1 or 0 to improve the prediction performance of the model.

[merge these paragraphs] Since the state vector, a, includes delay-coordinates, some matrix entries are known a priori and are independent of the dynamics. For example, the values of x_k should be mapped from their position in a_k to specific indices in a_{k+1}. Due to the least-squares fitting and coordinate transformation, DMDc will not produce these exact values in A and B. By forcing each of these matrix entries to 1 or 0, the state-prediction performance of the model is improved.

3.6. Implementation and results

3.6.1. Methodology

Simulation environment

Method overview   Maybe convert this to a flow diagram

1. Takeoff and hover

2. Command a series of velocity step inputs with random step sizes and time intervals

3. Measure and save input and output data

4. Apply algorithm to data and generate model

Steps and intervals   For the training period, different velocity step inputs are commanded with varying time intervals between step commands. A algorithm schedules these velocity step commands, by assigning random step values and time-intervals within a specified range. The velocity range is determined in simulation by iteratively increasing the maximum velocity step to a safe value where the quadrotor and payload system remain in stable flight. The maximum time-interval is set to a value that allows the payload swing to reach a steady-state condition. This ensures that the identified model includes transient and steady-state dynamics.

Why velocity steps?   Velocity step commands are used in the training period because this Frequency decomposition stimulates the system for a large range of frequencies.

Testing data

Error metric   Each state error signal is scaled by the reciprocal of the maximum value of that state variable in the training data. This is to ensure that a scale difference in the variable types create a bias in the error metric. For example, the quadrotor velocity reaches values of $3\,\text{m/s}$ but the payload swing angle has a maximum of only $0.526\,\text{rad}$. The velocity prediction error is therefore inherently larger than the payload angle prediction error and will bias the error metric towards favouring models with good velocity predictions. The proposed scaled error metric ensures that the MAE of each state variable can be compared to each other. It also provides an error metric that is better and unbiased representative of the model prediction performance across all state variables.

3.6.2. Hyperparameters

Fixed size of data Fixed sample time Fixed pendulum params Talk about the "front" Also about singular values For each of the experiments shown in this chapter, a hyperparameters selected tuned to produced

3.6.3. Sample time

best hyperparameters.

Fixed size of data. Fixed pendulum params.

3.6.4. Choice of payload variable in the state vector

As discussed in Section **??**, the continuous-time, equations of motion of a floating pendulum are dependent on $\dot{\theta}$ and V_N, but do not depend on θ. Therefore it is expected that $\boldsymbol{x} = \begin{bmatrix} V_N & \dot{\theta} \end{bmatrix}^T$ is used as the state vector for system identification. However, if $\dot{\theta}$ is not included in the state vector of a discrete model, it can still be represented with numerical differentiation like the backward Euler form,

$$\dot{\theta}_k = (\frac{1}{T_s}) \cdot \theta_k - (\frac{1}{T_s}) \cdot \theta_{k-1}. \tag{3.19}$$

Therefore the original state vector can also be replaced by, $\boldsymbol{x} = \begin{bmatrix} V_N & \theta \end{bmatrix}^T$ in system identification.

Based on the floating pendulum equations, it is expected that a model derived with $\dot{\theta}$ data will better approximate the actual dynamics than one using θ. This is because $\dot{\theta}$ contains more direct information about the dynamics compared to θ. A model using θ needs to "learn" numerical differentiation and the effect of $\dot{\theta}$ on the other variables. A model using $\dot{\theta}$ only needs to consider its relationship with other variables.
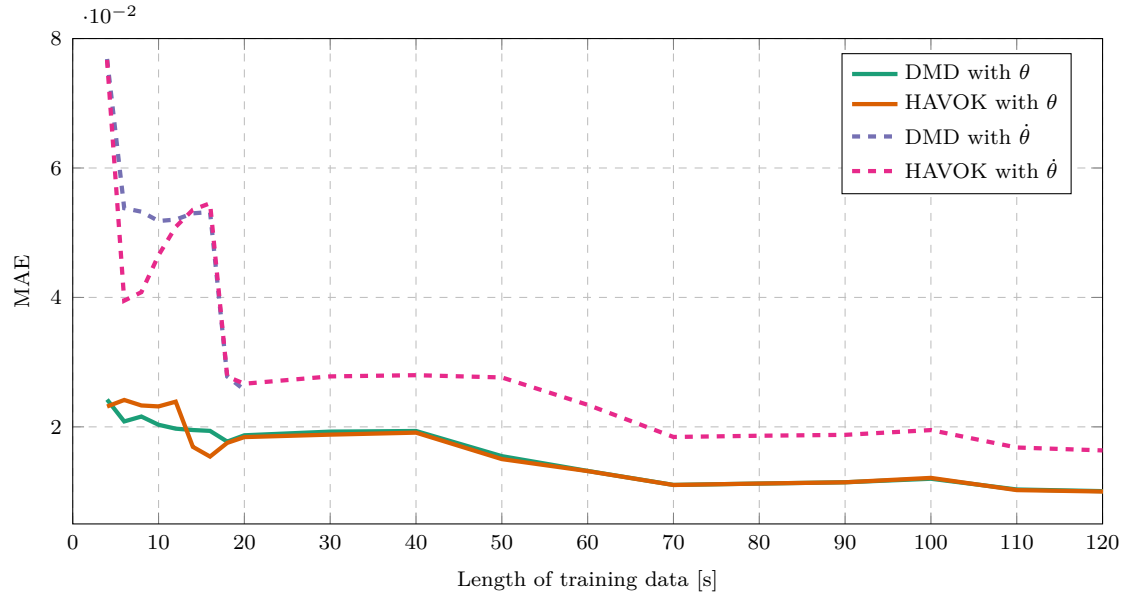
Figure 3.2: Prediction MAE for models using angle or angular rate measurements ($m = 0.2\,\mathrm{kg}$, $l = 0.5\,\mathrm{m}$, $T_s = 0.03\,\mathrm{s}$).

Figure **??** shows the prediction error of techniques using $\dot{\theta}$ or θ for different amounts of training data. For each length of training data, the hyperparameter combination producing the lowest prediction error was determined and used. From this plot it is clear that models with θ produce more accurate predictions than those with $\dot{\theta}$.

3.6.5. Noise

Measurement noise is Find reference for measurement noise definition This is bad for system identification because the output signals no longer represent the actual process hides the actual dynamics of the system under The IMU, barometer, magnetometer and GPS sensors on the practical quadrotor are used for state estimation and all experience measurement noise. The EKF performs sensor fusion and smooths out most of the measurement noise to provide a state estimate that is less noisy than raw sensor values.

The potentiometer and ADC which measure the payload angle on the quadrotor alos has quite a lot of measurement noise. However, this signal is not smoothed by an onboard EKF. Figure **??** shows the noisy payload angle measurement for a practical pendulum test while the quadrotor is held stationary. For models using θ in the state vector instead of $\dot{\theta}$, this noisy signal can be smoothed with matlab smoother. Figure **??** compares the noisy payload angle measurement to the smoothed signal and actual payload angle for a simulated flight. The is applied as band-limited white-noise and the noise power was iteratively adjusted to match that of the practical payload measurements.

However, since there is no direct measurement of $\dot{\theta}$, numerical differentiation is performed on the noisy θ measurement to estimate $\dot{\theta}$. This amplifies the noise and results in inaccurate $\dot{\theta}$ signal. Total variation differentiation is implemented to estimate $\dot{\theta}$ from the noisy measurements more accurately. [] Figure **??** shows

Noise also affects model prediction accuracy and the length of training data required for adequate predictions.

3.6.6. Size of training data

The length of training data used for system identification affects the quality of the model produced. In Figure **??** it is clear that prediction error decreases as the amount of training data increases. As more training data is used in the regression problem, the determined model better approximates the actual dynamics because a large range of the dynamics is "seen" by the algorithm.

Models produced from data lengths as short as $5\,\mathrm{s}$ predict the movement of state variables surprisingly well. Figure **??** shows prediction. Note how the general shape of the prediction represents the training data, even though it contains a lot more high frequency oscillations.

Figure **??** shows the MAE of prediction state derivative. Define MAE diff with equation **??**. From Figure **??** it appears that at least training data is required to produce models that represent the dynamics.

The models produced from HAVOK appear to produce slightly better prediction errors, however this small difference has a negligible effect on control performance.

In Figure **??** it can be seen that after approximately the prediction error does not significantly improve with more training data. It practice less training data is desirable because less flight time will be wasted on training a model before the quadrotor can fly with a updated controller. Less training data also corresponds to lower memory usage on quadrotor hardware. Such a slight improvement in prediction error also has a negligible effect on control performance and is therefore not worth the increased data requirement. Therefore, only of flight data will be used to train system identification models.

3.6.7. System parameters

Best hyperparameters. Fixed size of data. Fixed sample time.

3.6.8. Dynamic payload

Data-driven vs Parameter estimation

3.6.9. Practical flight data

3.6.10. HIL

Companion computer

Software

CPU

Memory

Chapter 4

Summary and Conclusion

Appendix A

Project Planning Schedule

This is an appendix.

Appendix B

Outcomes Compliance

This is another appendix.